Remote Sensing of Environment 121 (2012) 323–334

Contents lists available at SciVerse ScienceDirect

Remote Sensing of Environment

journal homepage: www.elsevier.com/locate/rse

Intercomparison of MODIS albedo retrievals and in situ measurements across the global FLUXNET network

Alessandro Cescatti [a,*], Barbara Marcolla [b], Suresh K. Santhana Vannan [c], Jerry Yun Pan [c], Miguel O. Román [d], Xiaoyuan Yang [e], Philippe Ciais [f], Robert B. Cook [c], Beverly E. Law [g], Giorgio Matteucci [h], Mirco Migliavacca [a], Eddy Moors [i], Andrew D. Richardson [j], Günther Seufert [a], Crystal B. Schaaf [k,e]

[a] European Commission — DG Joint Research Centre, Institute for Environment and Sustainability, Climate Change Unit, Ispra, Italy
[b] Fondazione Edmund Mach, IASMA Research and Innovation Centre, Sustainable Agro-ecosystems and Bioresources Department, 38010 S. Michele all'Adige, Italy
[c] Environmental Sciences Division, Oak Ridge National Laboratory, Oak Ridge, TN 37831, USA
[d] Terrestrial Information Systems Laboratory, NASA Goddard Space Flight Center, Greenbelt, MD, USA
[e] Center for Remote Sensing, Department of Geography and Environment, Boston University, 725 Commonwealth Avenue, Boston, MA 02215, USA
[f] Laboratoire des Sciences du Climat et de l'Environment (LSCE), Joint Unit of CEA-CNRS-UVSQ, Gif-sur-Yvette, France
[g] Department of Forest Ecosystems & Society, Oregon State University, Corvallis, OR, USA
[h] CNR-ISAFOM, Via Cavour, 4-6, 87036 Rende, CS, Italy
[i] ESS-CC, Alterra Wageningen UR, Wageningen, Netherlands
[j] Harvard University, Department of Organismic and Evolutionary Biology, Harvard University Herbaria, 22 Divinity Avenue, Cambridge, MA 02138, USA
[k] Environmental, Earth and Ocean Sciences, University of Massachusetts Boston, Boston, MA 02125, USA

ARTICLE INFO

Article history:
Received 18 October 2010
Received in revised form 7 January 2012
Accepted 18 February 2012
Available online 22 March 2012

Keywords:
MODIS
Surface albedo
Validation
FLUXNET
Terrestrial ecosystems
Plant functional types
Remote sensing

ABSTRACT

Surface albedo is a key parameter in the Earth's energy balance since it affects the amount of solar radiation directly absorbed at the planet surface. Its variability in time and space can be globally retrieved through the use of remote sensing products. To evaluate and improve the quality of satellite retrievals, careful intercomparisons with in situ measurements of surface albedo are crucial. For this purpose we compared MODIS albedo retrievals with surface measurements taken at 53 FLUXNET sites that met strict conditions of land cover homogeneity. A good agreement between mean yearly values of satellite retrievals and in situ measurements was found ($r^2 = 0.82$). The mismatch is correlated with the spatial heterogeneity of surface albedo, stressing the relevance of land cover homogeneity when comparing point to pixel data. When the seasonal patterns of MODIS albedo are considered for different plant functional types, the match with surface observations is extremely good at all forest sites. On the contrary, satellite retrievals at non-forested sites (grasslands, savannas, croplands) underestimate in situ measurements across the seasonal cycle. The mismatch observed at grassland and cropland sites is likely due to the extreme fragmentation of these landscapes, as confirmed by geostatistical attributes derived from high resolution scenes.

1. Introduction

Land surface broadband albedo directly affects Earth's climate by determining the fraction of shortwave radiation absorbed at the ground and therefore influencing the surface energy budget (Dickinson, 1983). Surface albedo is a crucial parameter in determining the magnitude of energy fluxes in the soil–plant–atmosphere continuum (Bonan, 2008; Chapin et al., 2008), affecting surface temperature, evaporation and transpiration, cloud formation and precipitation, thus ultimately impacting gross primary productivity (Dickinson, 1983; Lawrence & Slingo, 2004; Ollinger et al., 2008; Sellers et al., 1997). Several studies have investigated the interplay between albedo and drought (Govaerts & Lattanzio, 2008) or fires (Randerson et al., 2006), and the climate sensitivity to variation in surface albedo caused by major changes in land cover as the expansion of agricultural land in the northern hemisphere during the 18th century (Myhre et al., 2005; Vavrus et al., 2008). Surface albedo is also a key factor in the potential positive feedback between surface temperature and global warming at northern latitudes (Chapin et al., 2005) and may play a relevant role in offsetting the carbon sequestration potential of afforestation programs (Anderson et al., 2010; Betts, 2000; Betts et al., 2007; Bird et al., 2008; Rotenberg & Yakir, 2010).

Given the relevance of surface albedo in the Earth's climate system, monitoring this parameter in space and time is fundamental for the development of global climate models (Alton, 2009; Frida A-M et al., 2006; Hollinger et al., 2009; Tian et al., 2004) and for climate

* Corresponding author at: European Commission — DG Joint Research Centre, Institute for Environment and Sustainability, TP290, Via E. Fermi, 2749, I-21027 Ispra (VA), Italy. Tel.: +39 0332 78 5582; fax: +39 0332 78 5704.
E-mail address: alessandro.cescatti@jrc.ec.europa.eu (A. Cescatti).

0034-4257/$ – see front matter © 2012 Elsevier Inc. All rights reserved.
doi:10.1016/j.rse.2012.02.019

change and ecosystem research in general (Betts, 2000; Charlson et al., 2007; Charney et al., 1977; Dirmeyer & Shukla, 1994; Hall & Qu, 2006; Henderson-Sellers & Wilson, 1983; Pinty et al., 2011a). An important step toward the availability of global surface spectral albedo has been the launch of NASA's Terra and Aqua satellites and the MODerate-resolution Imaging Spectroradiometer (MODIS) (Lucht et al., 2000b; Salomonson et al., 1989; Schaaf et al., 2002). The MODIS sensor provides global maps of surface albedo reconstructed from retrieved models of reflectance anisotropy at a 500-m gridded spatial resolution every 16 days for the first seven MODIS spectral bands (0.47–2.1 μm) and for three broadband regions (0.3–0.7, 0.7–5.0, and 0.3–5.0, μm) (Lucht et al., 2000b; Moody et al., 2008; Schaaf et al., 2002).

Comparing satellite albedo retrievals with surface measurements and with independent satellite products is fundamental in evaluating the accuracy of remote sensing products and improving retrieval algorithms (Liang et al., 2002; Pinty et al., 2011b). Several recent studies have evaluated the consistency of global albedo products using in situ data at various spatial and temporal scales (Chen et al., 2008; Jin et al., 2003a, 2003b; Liang et al., 2002; Liu et al., 2009; Román et al., 2009, 2010; Wang et al., 2010) and under specific snow cover conditions (Stroeve et al., 2005). Most of these studies stress that a direct comparison is very challenging because of scale mismatch and heterogeneity of the land surface at the satellite measurement scale that reduces the spatial representativeness of ground point measurements (Liang et al., 2002; Román et al., 2009, 2010). As a consequence, a careful selection of ground points and the characterization of their spatial representativeness are crucial for a meaningful point-to-pixel comparison (Liang et al., 2002; Lucht et al., 2000a; Román et al., 2009).

Intercomparisons of surface and satellite albedo have been performed so far at a limited number of locations (Jin et al., 2003b; Liu et al., 2009; Román et al., 2009, 2010; Salomon et al., 2006; Wang et al., 2010) and a global analysis across different continents and plant functional types (PFTs) is still lacking. The objective of this work is to provide a comprehensive intercomparison in time and space of in situ measurements and satellite retrievals of snow-free broadband surface albedo. For this purpose we compared MODIS gridded albedo retrievals at the 500-m scale with ground measurements performed across the FLUXNET network (Baldocchi et al., 2001), the largest global data set of energy and mass flux measurements at ecosystem scale.

The geographical extent of the terrestrial data set allowed the comparison of several PFTs in a comprehensive and consistent way across the seasonal cycle. In addition, the large number of experimental sites in the network provided an unprecedented opportunity to perform a careful evaluation of the surface heterogeneity at the reference plots, based on a combination of qualitative and quantitative metrics. For this purpose images from MODIS, Google Earth, and Enhanced Thematic Mapper Plus (ETM+) have been used at various spatial scales (from 1×1 to 7×7 km). Differences between satellite retrievals and in situ albedo have been analyzed as a function of surface heterogeneity, PFT and seasonality. Results of the intercomparison have been finally discussed considering the different sources of uncertainty that affect the terrestrial and satellite datasets.

2. Materials and methods

2.1. Surface data set

In this study, we used in situ radiometric measurements available in the FLUXNET "La Thuile" database (www.fluxdata.org, October 2010) released in December 2007, which includes half hourly observations of ecosystem fluxes and meteorological data from more than 250 sites, for a total of 960 site-years.

Albedo is computed as the ratio of downward and upward global radiation as observed with double pyranometers (e.g. CMA-11, CMA-6 or CNR-1, Kipp&Zonen, Delft, The Netherlands). Surface albedo is typically estimated in the spectral range 280–2800 nm (accounting for more than 98.5% of the surface solar radiation according to ASTM G-173 reference spectra) and is therefore comparable with the broadband MODIS albedo (300–5000 nm). Giving that the field of view (FOV) of the pyranometers is typically 180°, the footprint of surface reflectance measurements is theoretically infinite. However, due to the cosine response of the sensor, 50% of the signal originates in a FOV of 90° and 80% in a FOV of 127°. The footprint of surface albedo therefore depends on the height of the albedometer above the canopy top (ranging from 5 to 10 m) and typically 80% of the signal originates within 10–20 m from the tower.

The uncertainty of surface albedo measurements depends on the absolute accuracy of pyranometers (about 5%) and on the non-ideal cosine response (about 3%). Most of the errors associated with the absolute accuracy of the instrument are similar for upward and downward fluxes and therefore compensate. Overall the expected accuracy is in the order of 4–7% in clear sky and 1–4% in overcast condition (Pirazzini, 2004; Pirazzini et al., 2006).

The geographical distribution of the sites is strongly clustered in Europe and North America (97 and 106 sites corresponding to 38% and 42% of the total), which are the regions with the longest history of continuous ecosystem flux measurements (Baldocchi et al., 2001). Several sites in the database are located in tropical Amazonia and East Asia, while the coverage in Africa, Central Asia, and Australia remains sparse and limited in the number of observation years. Despite the uneven geographical distribution, the "La Thuile" database guarantees a good coverage of the most important plant functional types, among which evergreen needle leaf forest (ENF), grassland (GRA), deciduous broadleaf forest (DBF), and cropland (CRO) are the most represented with respectively 28%, 18%, 13% and 12% of the sites.

Out of the 138 FLUXNET sites reporting continuous measurements of incoming and outgoing shortwave radiation, 18 have been excluded after a QA/QC analysis of the albedo data series. The QA/QC procedure was based on the following criteria: occurrence of an offset in the incoming or reflected radiation (night-time data systematically and significantly different from zero), occurrence of phase lag between incident and reflected radiation and systematic occurrence of unrealistic values (e.g. reflected radiation higher than incident radiation).

The land cover characteristics of the remaining 120 sites have been carefully classified using high resolution satellite images (available via Google Earth™), to identify those matching the requirement of homogeneity in the area surrounding the measurement tower (Jin et al., 2003b; Román et al., 2009, 2010). Although MODIS albedo is gridded at 500-m resolution, the land classification has been performed at 1 km^2, taking into account the uncertainty in the geospatial registration of satellite products and the fact that the albedo retrieval algorithm is based on multi-angle observations covering larger areas at the edge of the scan.

The classification process was based on the following four steps:

1 visual identification of the number and extension of different PFTs in the 1 km^2 area surrounding the tower;
2 verification of the correspondence between the dominant PFT in the 1 km^2 area and the PFT at the tower site as reported in the FLUXNET database;
3 qualitative ranking of landscape heterogeneity in three classes (low, medium, high) based on the plant canopy characteristics (tree density, patchiness, etc.);
4 attribution of a confidence level in the classification of the sites (low, medium, high) based on the quality of the image.

To guarantee the highest level of homogeneity and to minimize issues associated with spatial representativeness in the point-to-pixel comparison, only those sites characterized by the lowest level of

heterogeneity and with only one PFT in the 1 km^2 area were included in the analysis.

2.2. MODIS products

The MODIS albedo retrievals at the FLUXNET sites were generated using three MODIS products, namely, MCD43A1 (BRDF-Albedo Model Parameters 16-Day L3 Global 500 m), M*D04 (Aerosol product daily L2 Global 10 km), and MCD43A2 (BRDF-Albedo Quality 16-Day L3 Global 500 m). All these products are from the Collection V005 MODIS reprocessing campaign. The MODIS surface reflectance anisotropy and albedo product is based on all high quality, cloud-free, atmospherically corrected surface reflectances that are obtained over a 16-day period. When sufficient observations are available to adequately sample the surface anisotropy, an appropriate rendition of the RossThickLiSparse-Reciprocal Bidirectional Distribution Reflectance Model (BRDF) model is retrieved (Lucht et al., 2000b; Schaaf et al., 2002). This retrieval is attempted every 8 days at a 500 m gridded resolution. This retrieval model is used to generate intrinsic values of clear-sky direct surface albedo (referred to as directional hemispherical reflectance or black-sky albedo) and wholly diffuse albedo under isotropic illumination (bihemispherical albedo or white-sky albedo). These can be combined under particular illumination and atmospheric aerosol optical depth conditions (Lucht et al., 2000b; Román et al., 2010) to provide clear-sky albedos comparable to those measured in situ at a flux tower. Albedo quantities are reported at a 500-m gridded resolution, but all multi-angle observations that encompass areas are utilized in the retrieval. Therefore, although extended observation coverage is somewhat compensated for in the retrieval process, it is best to consider regions larger than 500 m when comparing observations made from satellite to those made on the ground. The stated accuracy of the high quality MODIS albedo retrievals (MCD43) in clear sky situations is 5%, as derived from the supporting studies listed at: landval.gsfc.nasa.gov/ProductStatus.php?ProductID=MOD43.

The calculation of clear-sky surface albedo at the tower sites involved the following two steps. The first step was the generation of the aerosol optical depth values for each site and each calendar date using the MODIS-Terra (MOD04) and MODIS-Aqua (MYD04) aerosol swath products. To generate the optical depth, the MODIS Adaptive Processing System — MODAPS (Masuoka et al., 2000, 2007) was used to prepare M*04 subsets at the 50×50 km region centered at the site. All pixels that had optical depth values greater than 0.35 or a cloud fraction greater than 0.6 were filtered out and not used in the optical depth generation. All pixels that had fill values for solar zenith angle were also rejected. After the filters were applied, a combined M[OY]D optical depth file was generated for each site, taking valid optical depth values from Terra and Aqua and generating one mean value for the optical depth per site per day. This method of course is not as accurate as having instantaneous sun photometer data (Holben et al., 1998) at the site, but the mean gives an approximation of the aerosol optical depth over the local solar noon.

The second step was the calculation of the clear sky surface albedo on the basis of the MODIS-derived 550 nm aerosol optical depths calculated in the previous step, the local solar zenith angle, the MCD43A1 product, and QA flags from MCD43A2 for each site involved in the analysis and for each date. If a date has no valid MCD43A1 pixels or if the optical depth was a fill value, no albedo was calculated for that date. As far as quality criteria are concerned only "full BRDF inversion" pixels (QA = 0 processed, good quality) were included in the calculation, while the "Snow_BRDF_Albedo" band of the MCD43A2 product was used to identify and exclude snow albedo retrievals. Following this procedure clear-sky MODIS albedo at local solar noon were retrieved at each FLUXNET site for all days with available aerosol MODIS product (M*D04) information, snow-free conditions, and solar elevation angles greater than 20°. On the same dates, the flux tower measurements of the albedo have been averaged for the hour centered at solar noon.

To integrate the observations at the FLUXNET sites in the global picture, snow-free global albedo averages per PFT and latitudinal band were computed from the MODIS V005 0.05 degree Climate Modeling Grid (CMG) product and stratified with the MCD12C1 land cover product. Yearly averages have been calculated on each pixel fulfilling the following requirements: QA = 0 (majority processed, good quality), snow coverage less than 10% (based on MODIS estimates), and major PFT coverage greater than 70% of the pixel. Note that the 0.05 degree MCD43C1 product is an average of the 500 m pixel underlying each 0.05 degree pixel and the quality flag only represents the quality of the majority of the underlying pixels.

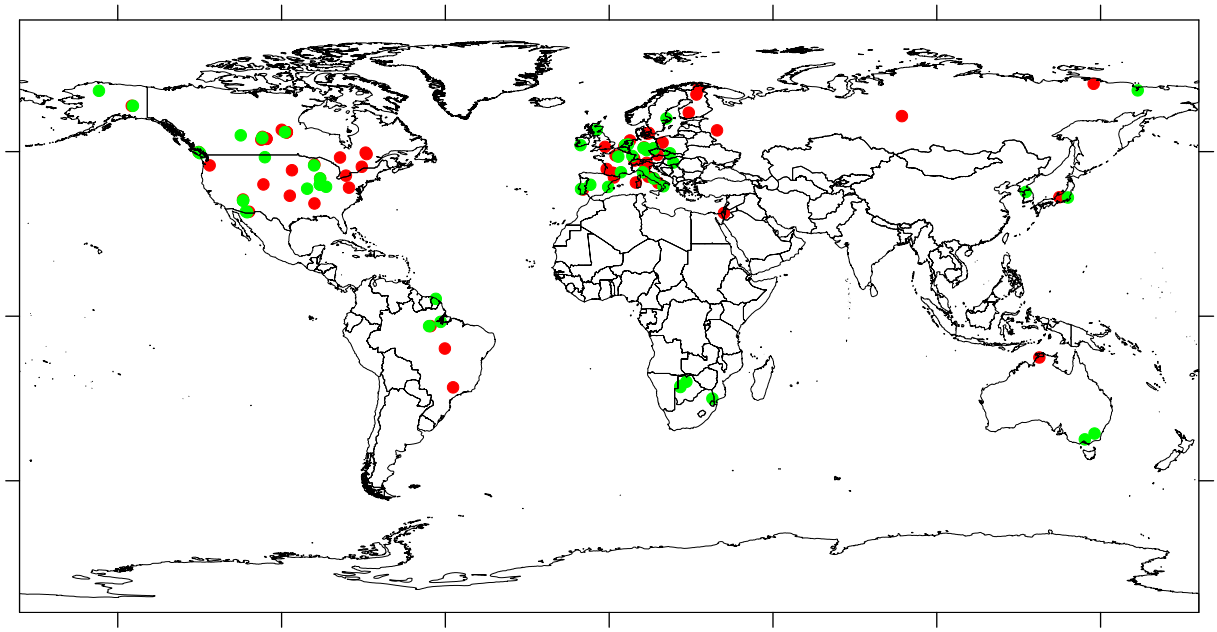

Fig. 1. Spatial distribution of the 120 FLUXNET sites for which albedo measurements are available. Green dots represent sites selected for the analysis according to plant cover homogeneity at a 1 km^2 scale (n = 53, visual classification based on high resolution Google Earth™ images, e.g. Fig. 2).

2.3. Landscape heterogeneity

One of the key issues in the intercomparison of satellite retrieval and surface observations is the objective and quantitative evaluation of landscape heterogeneity and the representativeness of in situ measurements (Liang et al., 2002; Román et al., 2009; Susaki et al., 2007).

For this purpose we applied the methodology presented by Román et al. (2009) based on the estimation of geostatistical attributes from high resolution scenes (Enhanced Thematic Mapper Plus). The spatial patterns and scales of landscape heterogeneity have been estimated from variogram models fitted at the FLUXNET sites over the spatial scales of MODIS observations.

In synthesis, the methodology adopted for the estimation of geostatistical indexes is based on the comparison of variogram model parameters retrieved at different spatial resolutions (i.e. from 1.0 km^2 to 1.5 km^2 squared subsets). By examining the variogram parameters at two scales, the spatial characteristics of a given measurement site is compared against the larger landscapes extending to several MODIS pixels.

Four different geostatistical attributes of spatial representativeness have been used to describe the overall variability (R_{CV}), spatial extent (R_{SE}), strength of the spatial correlation (R_{ST}), and spatial structure (R_{ST}) of surface albedo for a given measurement site. Further details on the methods and algorithms used to calculate these attributes are reported in Román et al. (2009).

Table 1
Characteristics of FLUXNET sites used in the analysis. N obs indicates the number of days of synchronous recordings of MODIS and in situ albedo. The averages of MODIS retrievals and in situ observations are reported in the two following columns. The two rightmost columns report the index of landscape heterogeneity (ST_{score}) derived from high resolution scenes (Enhanced Thematic Mapper Plus, when available) during the leaf-on and leaf-off seasons.

N	Site ID	Country	PFT	Lat. [deg]	Long. [deg]	N obs	MODIS albedo	In situ albedo	ST_{score} leaf-on	ST_{score} leaf-off
1	AU Tum	Australia	EBF	−35.66	148.15	733	0.11	0.11	9.75	
2	AU Wac	Australia	EBF	−37.43	145.19	275	0.09	0.1	11.3	
3	BR Cax	Brazil	EBF	−1.72	−51.46	67	0.12	0.12	5.33	
4	BR Sa3	Brazil	EBF	−3.02	−54.97	79	0.13	0.12	6.23	
5	BW Ghg	Botswana	SAV	−21.51	21.74	28	0.16	0.18	0.67	0.60
6	BW Ghm	Botswana	WSA	−21.2	21.75	28	0.18	0.17		
7	BW Ma1	Botswana	WSA	−19.92	23.56	252	0.16	0.14	5.42	3.40
8	CA Ca1	Canada	ENF	49.87	−125.33	580	0.09	0.09	5.99	
9	CA Ca3	Canada	ENF	49.53	−124.9	552	0.13	0.14	0.64	
10	CA NS6	Canada	OSH	55.92	−98.96	353	0.1	0.12		
11	CA SF2	Canada	ENF	54.25	−105.88	363	0.11	0.11	1.72	
12	CA SF3	Canada	ENF	54.09	−106.01	362	0.1	0.1	3.14	
13	CA WP1	Canada	MF	54.95	−112.47	353	0.11	0.13	1.65	1.15
14	CZ BK1	Czech Republic	ENF	49.5	18.54	148	0.09	0.1	3.18	
15	DE Geb	Germany	CRO	51.1	10.91	328	0.17	0.18	0.9	0.88
16	DE Hai	Germany	DBF	51.08	10.45	451	0.13	0.13	1.97	4.01
17	DE Kli	Germany	CRO	50.89	13.52	256	0.16	0.19	0.62	0.88
18	DE Tha	Germany	ENF	50.96	13.57	477	0.1	0.07	5.99	
19	DE Wet	Germany	ENF	50.45	11.46	375	0.07	0.05	1.55	
20	ES ES2	Spain	CRO	39.28	−0.32	298	0.14	0.13	0.91	1.04
21	ES LMa	Spain	SAV	39.94	−5.77	455	0.16	0.19	1.89	1.89
22	FR Fon	France	DBF	48.48	2.78	162	0.14	0.13	0.51	0.64
23	FR Hes	France	DBF	48.67	7.07	474	0.15	0.14	1.44	1.21
24	FR Pue	France	EBF	43.74	3.6	401	0.11	0.12	0.87	
25	GF Guy	French Guyana	EBF	5.28	−52.93	216	0.12	0.1	1.92	
26	HU Bug	Hungary	GRA	46.69	19.6	523	0.16	0.2	1.74	0.93
27	IE Dri	Ireland	GRA	51.99	−8.75	160	0.2	0.22	1.05	
28	IT Bon	Italy	ENF	39.48	16.54	174	0.1	0.08	2.43	
29	IT Col	Italy	DBF	41.85	13.59	183	0.14	0.15	2.6	0.71
30	IT SRo	Italy	ENF	43.73	10.28	512	0.08	0.09	3.1	
31	JP Mas	Japan	CRO	36.05	140.03	177	0.12	0.13	1.15	1.20
32	KR Kw1	Korea	MF	37.75	127.16	216	0.09	0.09	3.81	13.41
33	NL Ca1	Netherlands	GRA	51.97	4.93	369	0.17	0.22	1.03	0.95
34	NL Lan	Netherlands	CRO	51.95	4.9	108	0.17	0.18	1.44	1.41
35	NL Loo	Netherlands	ENF	52.17	5.74	404	0.11	0.09	1.4	
36	PT Esp	Portugal	EBF	38.64	−8.6	437	0.13	0.11	0.86	
37	RU Che	Russia	MF	68.61	161.34	104	0.15	0.16	0.54	0.44
38	SE Nor	Sweden	ENF	60.09	17.48	234	0.1	0.09	3.84	
39	UK Gri	UK	ENF	56.61	−3.8	15	0.1	0.09	1.48	
40	US Aud	USA	GRA	31.59	−110.51	1244	0.18	0.21	0.62	1.12
41	US Bn1	USA	ENF	63.92	−145.38	104	0.11	0.09	0.56	
42	US Bo1	USA	CRO	40.01	−88.29	721	0.16	0.19		1.48
43	US Bo2	USA	CRO	40.01	−88.29	289	0.16	0.19		1.58
44	US Fmf	USA	ENF	35.14	−111.73	247	0.1	0.12	3.08	
45	US FPe	USA	GRA	48.31	−105.1	775	0.15	0.16	1.05	0.93
46	US Fuf	USA	ENF	35.09	−111.76	231	0.1	0.13	1.72	
47	US IB1	USA	CRO	41.86	−88.22	349	0.15	0.16	0.76	0.77
48	US Ivo	USA	WET	68.49	−155.75	62	0.18	0.19		
49	US MMS	USA	DBF	39.32	−86.41	639	0.13	0.13	8.75	6.87
50	US MOz	USA	DBF	38.74	−92.2	563	0.12	0.11	2.17	3.17
51	US SRM	USA	WSA	31.82	−110.87	826	0.17	0.16	2.13	1.48
52	US WCr	USA	DBF	45.81	−90.08	487	0.14	0.15	1.82	2.94
53	ZA Kru	South Africa	SAV	−25.02	31.5	447	0.15	0.15	1.34	1.28

Using a weighted combination of the four geostatistical attributes a comprehensive metric of the landscape heterogeneity (ST_{score}) has been computed to evaluate and compare FLUXNET sites:

$$ST_{score} = \left(\frac{|R_{CV}| + |R_{ST}| + |R_{SV}|}{3} - R_{SE}\right)^{-1}.$$

In addition, the landscape heterogeneity at a larger spatial scale (7×7 km) has been quantified as the standard deviation of MODIS albedo (14×14, 196 pixels) area centered at the FLUXNET site.

3. Results and discussion

3.1. The terrestrial data set: spatio-temporal distribution and representativeness

As a result of the visual classification of land cover characteristics, 49% of the 120 sites performing reliable continuous measurements of broadband albedo were rejected for reasons of landscape heterogeneity and 7% because of low confidence in the PFT classification.

Of the remaining 53 sites (among which there were 15 ENF, 8 CRO, 7 DBF, and 7 evergreen broad-leaf forests (EBF)) the largest fraction is located in Europe (19) and North America (15 USA, 7 Canada). The remainder of the sites are located in Africa (4), South America (3), Asia (3) and Australia (2) (Fig. 1, Table 1).

Across all sites, 18,666 days of synchronous MODIS retrievals and in situ surface albedo were available. On average, this worked out to 333 and 400 days of data for each forested and non-forested site, respectively (on average about 80 observations per site and year), but there was considerable variability among sites. To date, this is the largest data set that has been used to compare satellite and in situ albedo measurements.

Although the data set spans in the years 2000–2007, the vast majority (87%) of the observations were made between 2003 and 2006 (Fig. 2a). Because of filtering for snow and cloud cover, and the dominance of northern hemisphere sites in the data set, the number of observations is lower during winter months (November through February) (Fig. 2b).

The seasonal variation of the global average of snow-free albedo is remarkably small for forests, likely because ~70% of the sites are evergreen forests with leaf area index, canopy structure and chemistry that are not as dynamic as those of deciduous ecosystems. The seasonal trend of snow-free albedo is somewhat more pronounced for non-forest ecosystems, which include crops and grasslands (Running et al., 1995) (Fig. 2b).

The spatial representativeness of the FLUXNET albedo data set in the global albedo domain has been explored by superimposing the MODIS retrievals at the sites on the global distribution of MODIS albedo (Fig. 3) for the same PFT or latitudinal class. Concerning the latitudinal distribution, 75% of the FLUXNET sites are clustered in the 30–55° N band (Fig. 3a), and in this latitude band the surface albedo observed at the sites is substantially lower (20%) than the MODIS latitudinal average. This is due to the non-representative distribution of FLUXNET sites, which are mostly located in dense and productive temperate forests of the northern hemisphere. The difference between latitudinal MODIS averages and site-measurements of the

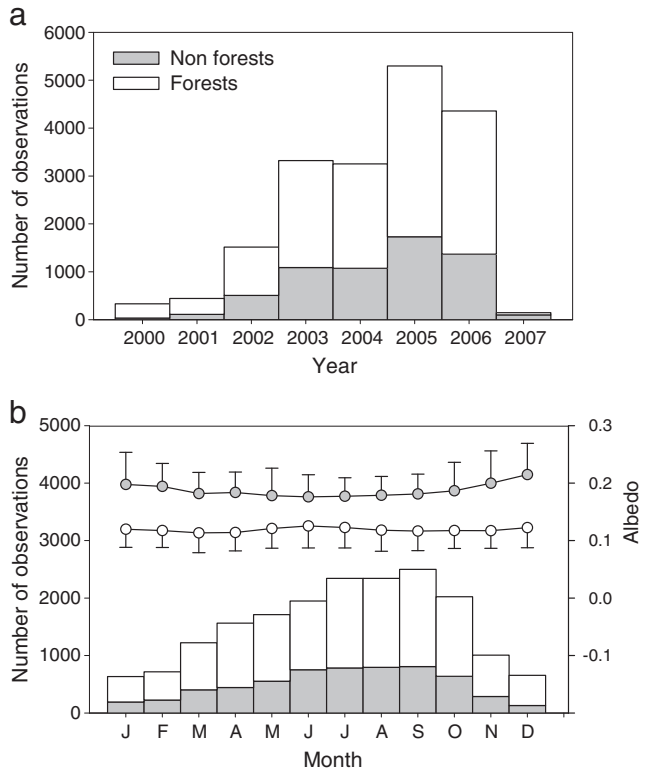

Fig. 2. Frequency distribution of synchronous MODIS retrievals and in situ measurements classified according to year (panel a) and month (panel b) of observation. The vegetation is coded according to the IGBP classification: CRO, croplands; CSH, closed shrublands; DBF, deciduous broad-leaf forests; EBF, evergreen broad-leaf forests; ENF, evergreen needle-leaf forests; GRA, grassland; MF, mixed forests; OSH, open shrublands; SAV, savannas; WET, permanent wetlands; WSA, woody savannas. Validation sites are separated into forests (ENF, EBF, DBF, MF, SAV and WSA) and non forests (OSH, CSH, CRO, GRA, WET).

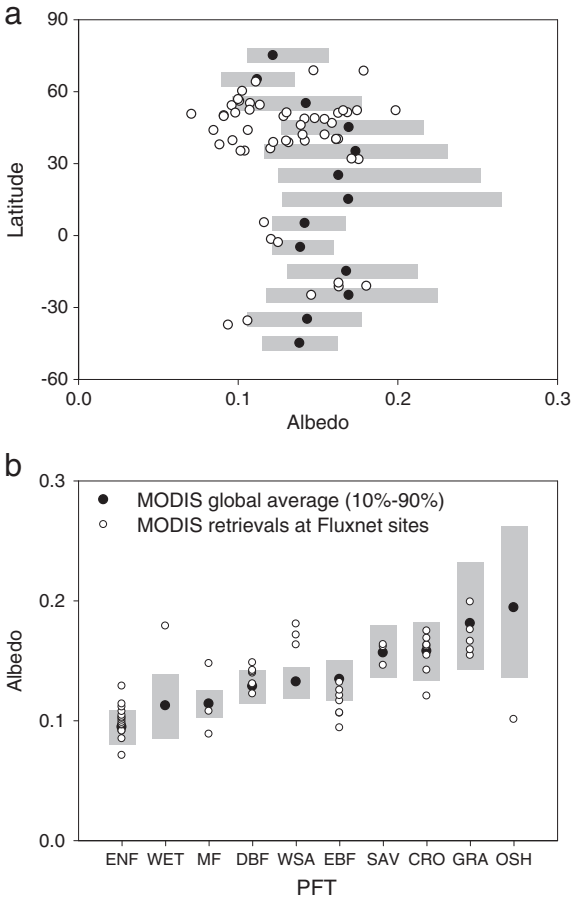

Fig. 3. Global distribution of MODIS albedo (0.05° res.) categorized for latitudinal bands (panel a) and plant functional types (panel b). In both panels black dots represent global MODIS averages (gray bars show the 10–90 percentile intervals) and white dots represent MODIS retrievals at the 53 FLUXNET sites reported in Table 1.

albedo is less evident in the southern hemisphere, where the number of FLUXNET site is remarkably lower.

In terms of PFTs (Fig. 3b), 79% of sites analyzed here are classified as one of ENF, EBF, CRO, GRA or DBF. When PFT averages are compared with the global PFT averages of MODIS albedo, most of the sites fall within the 10–90 percentile intervals of the global MODIS observations, with the exception of EBF for which MODIS retrievals at the sites show lower values of albedo. For the other PFTs (woody savanna (WSA), open shrubland (OSH), savanna (SAV), mixed forest (MF)) the number of sites is too low to speculate on the global representativeness of the FLUXNET dataset.

3.2. Point to pixel comparison

The comparison of MODIS albedo retrievals with in situ measurements has been limited to the FLUXNET sites with the highest degree of homogeneity in order to minimize the effect of the scale mismatch. Examples of high resolution images (available via Google Earth™) used to evaluate site homogeneity are reported in Fig. 4 for four test sites.

The time series of MODIS retrievals and in situ measurements at these four sites show contrasting results (Fig. 5). At some sites, the match is extremely good both in terms of absolute values and seasonal trend (e.g. US-MMS, US-FPe). At the other two locations MODIS retrievals show a systematic overestimation (e.g. PT-Esp) or underestimation (e.g. ES-LMa) of surface measurements. These biases are probably due to the fine-scale spatial variability of the plant cover and to the representativeness of the tower footprint in the MODIS pixel, since the other sources of uncertainties (sensor calibration, uncertainty of AOD estimates, etc.) cannot explain such large and systematic errors. In particular at sites with discontinuous plant canopies like ES-LMa (Fig. 4), the height from the ground and the spatial location of the albedometer are critical factors, determining the representativeness of the in situ measurements at the resolution of the satellite pixel.

A good agreement between satellite and in situ measurements was found when sites were grouped according to PFT (Fig. 6a, type II regression, $r^2 = 0.82$). Forest PFTs (such as ENF, EBF, MF) fall in the lower part of the graph, while non-forest PFTs (such as CRO, GRA, wetlands (WET)) fall in the upper part. Albedo is correlated to several plant-level traits including leaf albedo, leaf area index, vertical angle of leaves/needles, the degree of foliage and canopy clumping, and the geometric-optical shadowing due to canopy structure. It is well known that the structural canopy traits typical of tall canopies trap more of the incoming radiation, therefore reducing the canopy albedo of forest PFTs (Cescatti, 1998; Davidson & Wang, 2004).

Satellite retrievals and surface measurements at the site level (Fig. 6b) show a coefficient of determination of 0.83, very similar to that observed in the comparison by PFT and reported in other studies (Wang et al., 2010). Regressions in Fig. 6b show a positive intercept and slope lower than one (0.74) indicating a systematic low bias in the MODIS retrievals at sites with high albedo and an opposite bias at sites with low albedo. These differences may be primarily due to the different spatial scales of the two estimates, with satellite retrievals referring to a considerably larger area than tower measurements. The spatial averaging of surface albedo on the large MODIS pixels dampens the variability when compared with high-resolution imagery or point measurements and may ultimately determine the trend (intercept > 0 and slope < 1) of the regressions in Fig. 6. Similar slope and closer correlations have been observed by comparing early

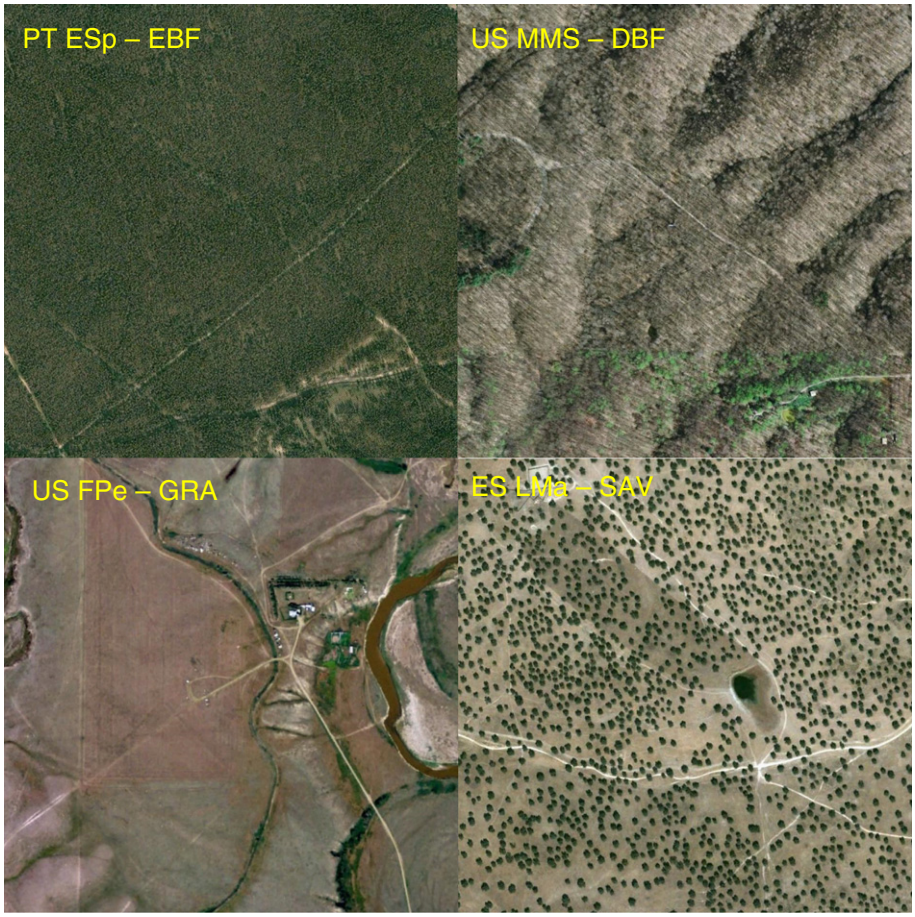

Fig. 4. Examples of high resolution Google Earth™ images used to visually classify the FLUXNET sites according to land cover homogeneity. Images cover an area of 1 km^2 centered at the tower coordinates.

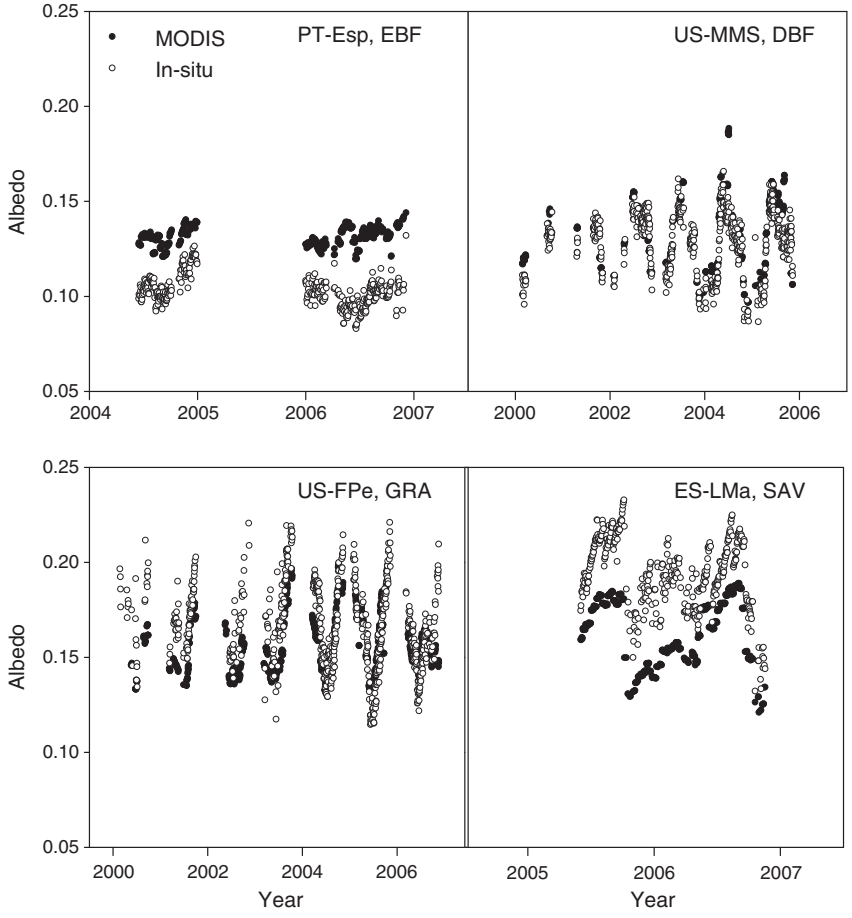

Fig. 5. Time series of synchronous in situ observations (open dots) and MODIS retrievals (black dots) at the four sites shown in Fig. 4.

MODIS retrievals with surface measurements using high-resolution remotely sensed imagery (Landsat7 ETM+) to characterize the land cover heterogeneity in the MODIS pixel (Liang et al., 2002).

The quantitative assessment of the spatial heterogeneity is reported in Fig. 7, according to the methodology proposed by Román et al. (2009). The leaf-on values of the geostatistical index proportional to landscape homogeneity (ST_{score}) are plotted against the mean error of satellite retrieval versus surface albedo. Despite the spread of the ST_{score} the following aspects are evident:

- Forest sites present a larger variability of STscore than the non forest sites, with locations either in the low or high range of spatial homogeneity. On the contrary herbaceous systems (GRA, CRO, SAV) are typically characterized by a ST_{score} lower than 2.
- In all PFTs, sites with the largest mean error show low values of ST_{score}, generally below 2.

These findings confirm the importance of landscape heterogeneity in the point to pixel inter-comparison and the validity of geostatistical indexes for the quantitative characterization of spatial patterns from high resolution scenes.

The mean error and mean absolute error of the MODIS retrievals vs. the in situ observations are reported in Fig. 8a together with the r^2 of the regression computed for the single sites. The mean error is a measure of the retrieval accuracy and is on average very small (−0.004), implying that the magnitude of the MODIS surface albedo is very similar to the in situ observations. It is also interesting to notice that the spread is considerably larger among the sites with a negative error both in terms of mean error and mean absolute error. The r^2 observed at single sites, proportional to the dot size in Fig. 8a, is largely independent of the mean error since it mostly depends on the seasonal variability of the measurements. For this reason, sites with a marked seasonality in albedo (i.e. deciduous forests, crops and boreal ecosystems) typically show a higher r^2 than tropical or Mediterranean evergreen forests.

The error distribution peaks in the −0.01 class and is skewed to the left, with larger errors at sites where MODIS underestimates surface measurements (Fig. 8b). The mean values of ST_{score} in the different classes of mean error show several interesting features (Fig. 8b). The mean value of the score peaks in the class at zero mean error (3.9). Score values are considerably lower (1–1.4) at sites characterized by a negative error (MODIS < in situ) with a rather limited variability between sites. At these sites the towers are probably located in a brighter spot than the average of the pixel and typically pertain to the categories of grassland (GRA) or cropland (CRO). On the contrary sites with a positive bias (MODIS > in situ albedo), where the tower spot is located on an area darker than the surroundings, show intermediate value of the score (2.5) and a large variability between sites.

Giving that the MODIS albedo product is reported at a 500 m resolution while the retrieval algorithm is based on multiangular reflectances that extend over this area, landscape heterogeneity at scales larger than 500 m may ultimately affect the uncertainty in the retrievals. To assess the impact of the spatial heterogeneity on the accuracy of MODIS retrievals we computed the mean absolute percentage error for site ensembles at increasing levels of spatial variability (expressed as standard deviation of MODIS albedo in the 7×7 km^2 area surrounding the site or as ST_{score}). We expressed the error as percentage since there is a factor two in the absolute value of the albedo between the darker (ENF) and the brightest PFTs (GRA). Fig. 9 shows that the error between satellite and in situ measurements

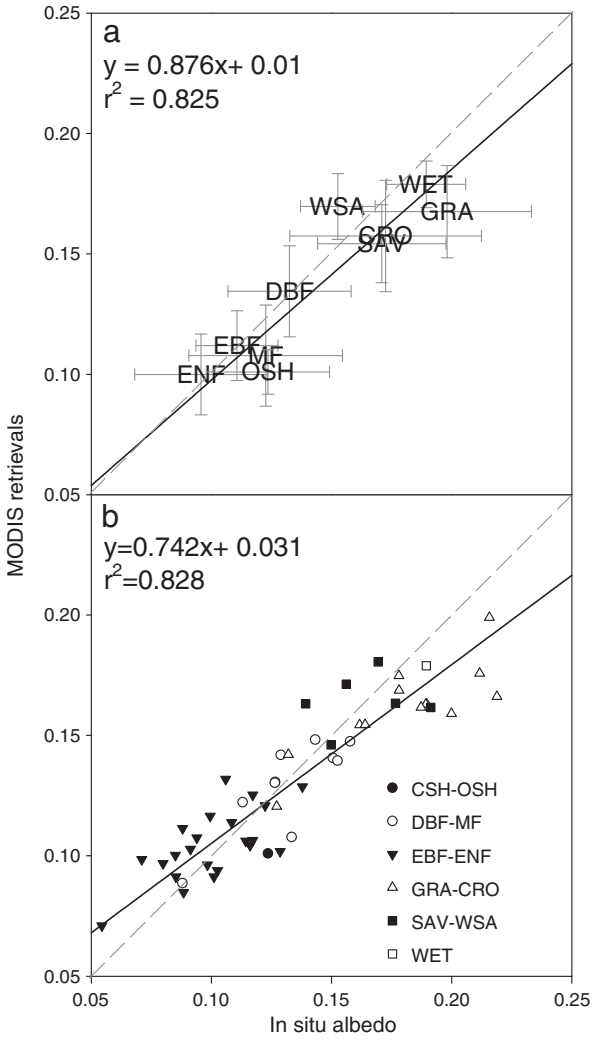

Fig. 6. MODIS retrievals versus in situ observations of clear-sky and snow-free albedo. a) Averages and standard deviations of retrievals (temporal and spatial variability are accounted for) grouped by plant functional types (PFT), b) average ground measurements and retrievals at individual sites classified by PFT.

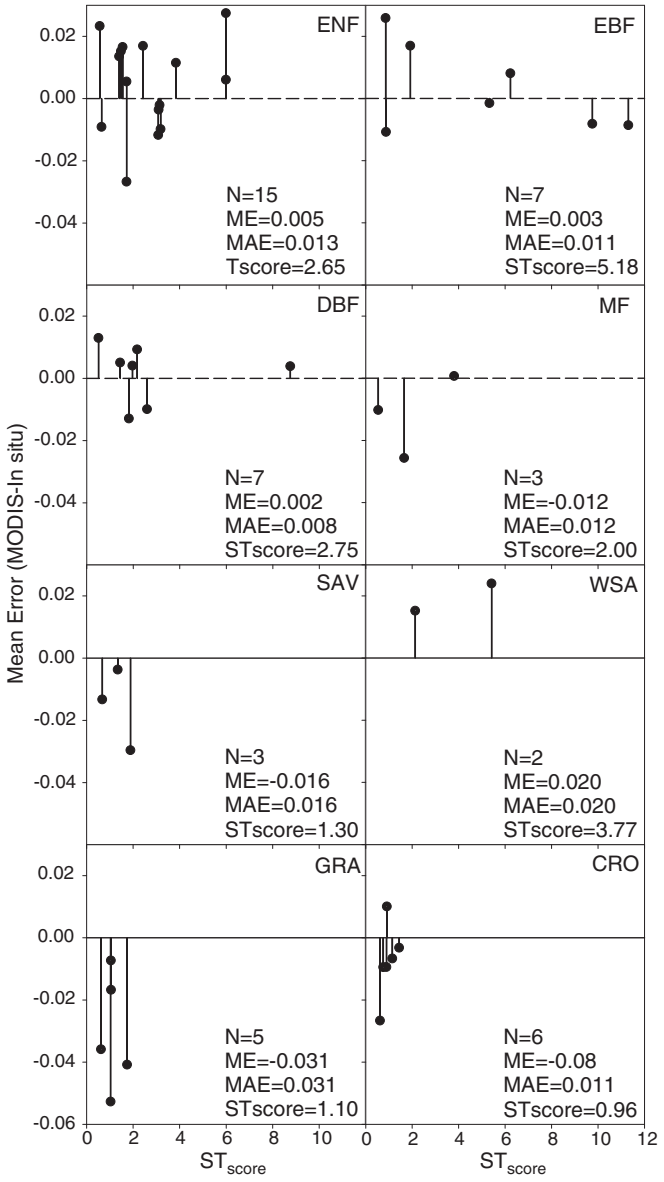

Fig. 7. Site index of landscape heterogeneity (ST_{score}) during the leaf-on season as derived from high resolution scenes (Enhanced Thematic Mapper Plus). ST_{score} statistics by PFT are reported in the single panels.

increases with the spatial variability of the albedo, further demonstrating the crucial issue of the spatial variability of surface albedo in the point to pixel intercomparisons.

Both the MODIS standard deviation and ST_{score} show sharp variations for values of the mean absolute percentage error of up to 12%. Above this threshold both indexes are no longer correlated with the error. The trend of the two spatial indexes is remarkably similar though in opposition, since MODIS standard deviation increases with the spatial variability while ST_{score} increases with spatial homogeneity. Despite the different spatial domains (7×7 and 1.5 km) the two indexes are strongly correlated (Fig. 9 inset) with an r^2 of 0.90. These results demonstrate that a close match between surface measurements and satellite retrievals is achievable only at the most spatially homogenous sites, where the canopy optical properties are scale-invariant. These golden sites can be effectively detected with both statistical analysis of MODIS albedo or with higher resolution images and detailed geostatistical indexes.

3.3. Seasonal trends

Seasonal patterns in the relationship between site-level averages of MODIS and FLUXNET albedo are reported in Fig. 10. In all seasons, the relationship between MODIS (y axis) and in situ (x axis) albedo has a slope ranging from 0.71 to 0.74 and a positive intercept, meaning that MODIS over-estimates surface albedo of low-albedo sites, and under-estimates albedo of high-albedo sites. These trends are largely driven by sites pertaining to CRO and GRA that are strongly underestimated in any season other than summer. The seasonality in CRO and GRA is modulated by the combined effect of climatic drivers and management practices and its retrieval is complicated by the typical landscape fragmentation of these PFTs.

The lowest correlation ($r^2=0.73$) is observed for winter values (from December to February) and the highest ($r^2=0.82$) for fall values (from September to November). Similarly, larger differences between in situ and satellite retrievals of surface albedo in winter season were observed in Jin et al., (2003b), who suggested that this was the result of the increased heterogeneity of surface reflectivity due to the presence of residual snow and canopy heterogeneity.

The inset in Fig. 10a shows the correlation matrix of the errors observed in the different seasons. All correlation coefficients are positive, meaning that sites with surface measurements larger than satellite retrievals in one season tend to have the same behavior in

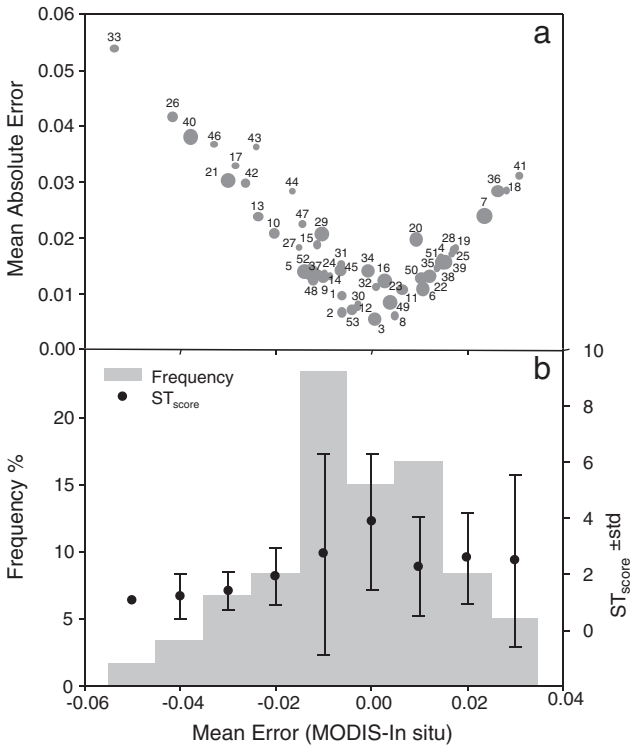

Fig. 8. a) Mean error and mean absolute error of MODIS albedo retrievals at FLUXNET sites. Site numbers are reported in Table 1; dot size is proportional to the r^2 of the regression of daily MODIS retrievals versus in situ measurements. b) Frequency distribution of the mean error (MODIS–in situ albedo at site level) and mean value of the landscape heterogeneity index (ST_{score}) for classes of mean error.

the other seasons. Thus, site-specific biases are coherent over time, possibly indicating mismatches between the footprint of tower radiometric instruments and the corresponding MODIS pixel, calibration errors of the tower radiometric instruments, inappropriate estimation of aerosol optical depths or systematic errors in MODIS retrieval.

In Fig. 11 the seasonal trends of satellite and in situ data for a set of PFTs are reported with their standard deviation, and superimposed on the range of MODIS albedo observed at the global scale for the same PFTs (gray bands represent the 10–90 percentile interval). An exceptionally good agreement between the two independent albedo estimates is observed for forest PFTs, both in terms of absolute albedo values and seasonal patterns. In contrast, for non-forest PFTs (CRO and GRA) MODIS retrievals are systematically smaller than surface measurements, while their respective seasonal patterns are in agreement as observed also by Davidson and Wang (2004). The mismatch observed at the non-forest sites is likely due to the extreme fragmentation of these landscapes and to the very limited spatial footprint of surface radiometric measurements performed at these sites (i.e. over short vegetation albedometers are typically installed few meters above the ground). Wang et al. (2010) reported that the average negative bias of MODIS albedo is probably due to the underestimation of visible surface reflectance and that this phenomenon may be more pronounced for herbaceous canopies with larger albedo in the visible bands.

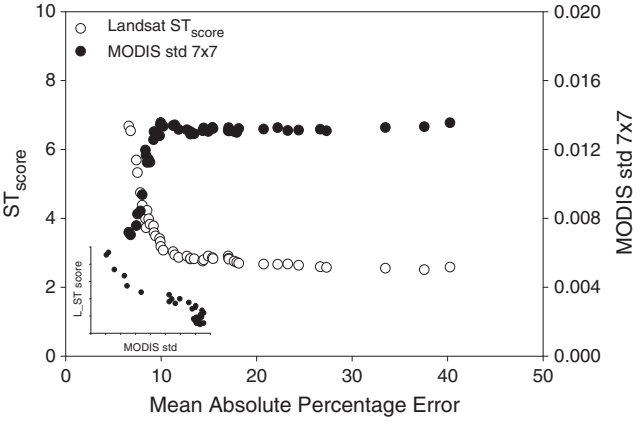

Fig. 9. Mean absolute percentage error of MODIS retrievals versus in situ measurements as a function of the 1) standard deviation of MODIS retrievals in the 7×7 km grid centered at the site and 2) of the heterogeneity index ST_{score}. Sites located in a more homogeneous landscape (lower spatial variability of albedo, higher ST_{score}) show a lower discrepancy between in situ observations and satellite retrievals.

The large variability of CRO and GRA surface albedo (Fig. 11) can be ascribed to the spatial variability in LAI, to the variable amount of exposed soil and soil moisture content, to the rapid temporal dynamic of the canopy in response to climatic drivers like temperature and water status (Gao et al., 2005) as well as to management practices (e.g. planting, harvesting, grazing, crop type, etc.) (Tittebrand et al., 2009). Given the large spatial variability of GRA and CRO albedo, future intercomparison of satellite and in situ observations for these PFTs should be performed preferentially at selected sites with homogenous crop cover and management practices at the MODIS spatial resolution.

ENF and EBF snow-free albedo do not show any significant seasonal trend and monthly values are around 0.1. EBF do not show seasonal variation also at the global scale, while larger variability is observed for ENF in winter months. A clear seasonality is shown by DBF + MF and CRO, with higher values at the peak of the growing season, in line with the results of other in situ studies (Sellers et al., 1997). The seasonal pattern of GRA is the opposite, with a winter maximum in albedo. The increase of GRA albedo from August, observed both in MODIS and FLUXNET data, is probably due to vegetation senescence, with the increase of exposed soil and dead biomass and the drying of stalks and seeds during summer months.

4. Conclusions

Surface albedo is a key parameter in the Earth's energy balance since it affects the amount of solar radiation directly absorbed at the planet surface. Its variability in time and space can be retrieved through the use of remote sensing products, available nowadays at high temporal and spatial resolution from different satellite platforms (e.g. Terra and Aqua MODIS observations are used to retrieve albedo every 16 days at a spatial resolution of 500×500 m starting March 2000).

Careful intercomparisons with in situ measurements of surface albedo are crucial to evaluate and improve the quality of remote sensing products. In this context, the “La Thuile” FLUXNET dataset offers an unprecedented opportunity to select sites according to strict conditions of landscape homogeneity and across a wide range of PFTs and geographical areas. When compared to the latitudinal distribution of surface albedo, the FLUXNET data set clearly shows a bias toward darker vegetated areas in the northern hemisphere. In this respect, the biased distribution of the terrestrial dataset in the global albedo domain should be taken into account when using in situ FLUXNET albedo data in the parameterization of land surface models.

The key issue in the intercomparison of satellite and in situ measurements is the spatial representativeness of the latter in the satellite pixel. The MODIS pixel can be 100–1000 times larger than the footprint of in situ radiometric observations, depending on the height of the albedometer above the canopy top. For this reason a careful classification of FLUXNET sites has been performed to select only those sites with the lower level of heterogeneity. Albedo measurements at the sites passing the selection criteria are in excellent agreement for most forest sites, while satellite retrievals underestimate in

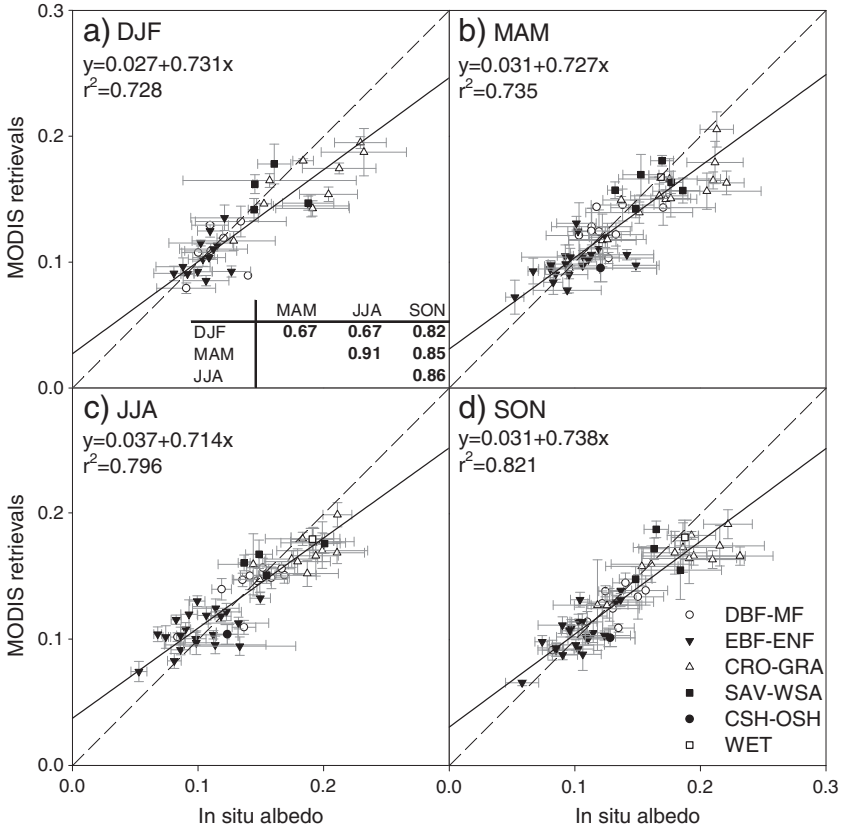

Fig. 10. Seasonal average values of clear-sky snow-free albedo at the 53 homogeneous sites as observed at the FLUXNET sites or retrieved from MODIS. Winter values (DJF) show the lowest correlation. The first panel includes the correlation matrix of the residuals (MODIS retrievals–in situ albedo) in the four seasons.

situ measurements for the PFTs with larger values of albedo (typically non-forest ecosystems as CRO and GRA).

When seasonal patterns of MODIS albedo are compared, the match is extremely good for all forest PFTs. These results quantitatively document the quality achieved with satellite retrievals of surface albedo over a range of forest ecosystems. To the contrary, satellite retrievals for non-forest sites systematically underestimate in situ measurements across the whole seasonal cycle with a minimum error at the peak of the growing season. However, in the interpretation of these results it should be considered that the footprint of the surface radiometric measurements is extremely limited in these ecosystems, since sensors are generally installed few meters above the ground. In addition the temporal and fine-scale spatial variability of the canopy reflectance can be extremely large in non-forest PFTs due to management practices and rapid LAI dynamics (Tittebrand et al., 2009).

The intercomparison of surface measurements and satellite retrievals is affected by the surface heterogeneity at various spatial scales. The sub-pixel variability affects the difference between the signal in the footprint of the albedometer and the 500 m MODIS pixel, while the between pixel variability affects the accuracy of the inversion algorithm. At a smaller scale, the combination of quantitative indexes based on variogram analysis of high resolution images confirms that FLUXNET sites in herbaceous ecosystems (CRO and GRA) are less homogenous and should therefore be carefully evaluated in point to pixel intercomparisons. At a coarser scale, the variability of the MODIS albedo in the 7×7 km^2 area is related to the mismatch of MODIS retrievals and in situ measurements, further corroborating the relevance of large scale landscape homogeneity in the comparison of surface measurements and satellite retrievals.

The results of this investigation clearly show the need to characterize the spatial heterogeneity of reference sites using a combination of surface measurements, and airborne and finer scale satellite imagery (Román et al., 2009). To overcome the limitations of the point to pixel albedo inter-comparisons, future field and airborne surveys should be planned to address the issue of spatial scales and landscape heterogeneity. Current approaches for measuring in situ albedo are not adequate to describe mixed or highly heterogeneous landscapes such as mixed forests, open shrublands, savannas and croplands. For this purpose only spatially-distributed measurements (i.e., airborne laser scanning, network of tall towers) could produce observations at the required scale. For albedo in particular, multi-angle airborne instruments such as AirMISR (Diner et al., 1998), AirPOLDER (Chen et al., 1997), NASA's Cloud Absorption Radiometer (Gatebe et al., 2003) and the Compact Airborne Spectrographic Imager (CASI) data (Chen et al., 1999) could be effectively used to retrieve surface-level bidirectional reflectance measurements at a landscape scale and therefore effectively complement moderate resolution satellite systems like MODIS and MISR.

Acknowledgments

This work is based on radiometric measurements acquired by the FLUXNET community and in particular by the following networks: AmeriFlux (US Department of Energy, Biological and Environmental Research, Terrestrial Carbon Program (DE-FG02-04ER63917 and DE-FG02-04ER63911)), AfriFlux, AsiaFlux, CarboAfrica, CarboEuropeIP, CarboItaly, CarboMont, ChinaFlux, FLUXNET — Canada (supported by CFCAS, NSERC, BIOCAP, Environment Canada, and NRCan), GreenGrass, KoFlux, LBA, NECC, OzFlux, TCOS — Siberia, and USCCC. We

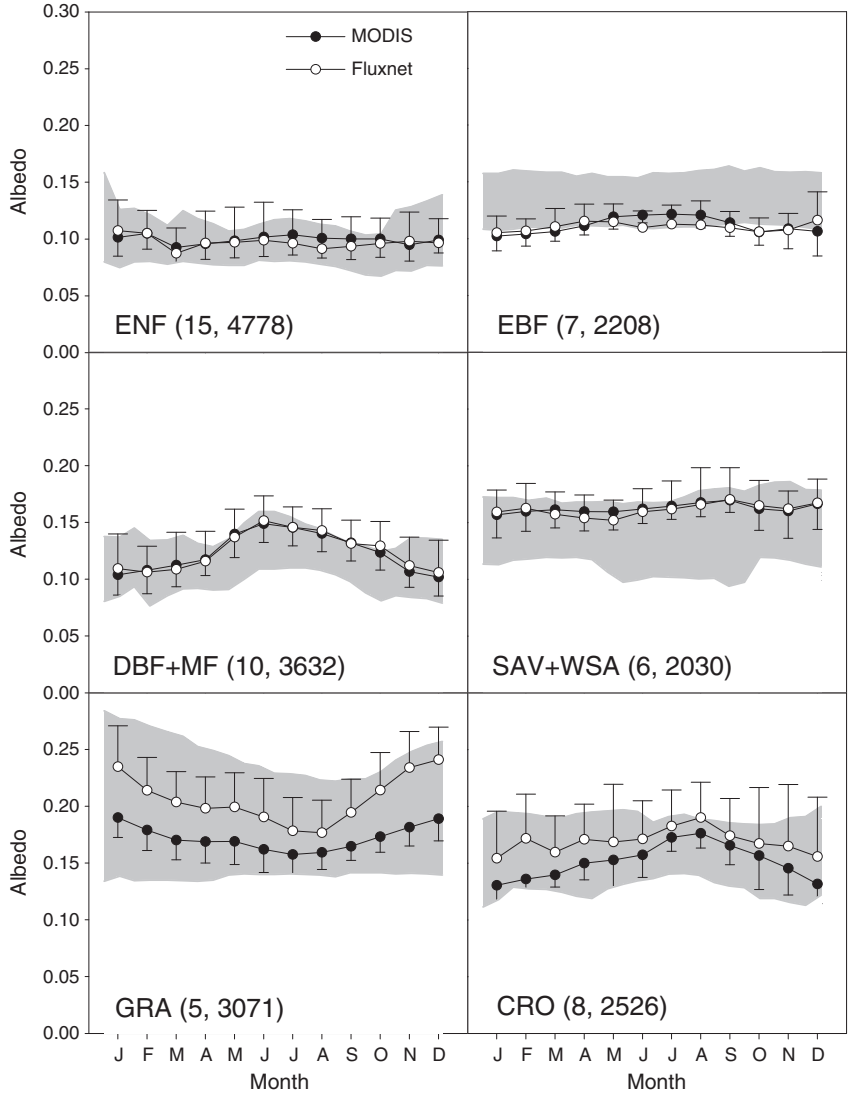

Fig. 11. Seasonal trends of albedo for the different plant functional types as derived from in situ observations (white dots) and MODIS retrievals (black dots). The gray bands show the observed variability (10–90 percentiles) of the MODIS retrieved albedo at a global scale for each plant functional type.

acknowledge the support to data harmonization provided by CarboEuropeIP, FAO-GTOS-TCO, iLEAPS (the Integrated Land Ecosystem-Atmosphere Processes Study, a core project of IGBP), Max Planck Institute for Biogeochemistry, National Science Foundation, University of Tuscia, Université Laval and Environment Canada and US Department of Energy and the database development and technical support from Berkeley Water Center, Lawrence Berkeley National Laboratory, Microsoft Research eScience, Oak Ridge National Laboratory, University of California — Berkeley, and University of Virginia. The processing of MODIS data has been supported by NASA grant NNX08AE94A. Support for C. Schaaf and X. Yang was provided by NASA grant NNX08AE94A.

References

Alton, P. (2009). A simple retrieval of ground albedo and vegetation absorptance from MODIS satellite data for parameterisation of global land-surface models. *Agricultural and Forest Meteorology*, *149*, 1769–1775.

Anderson, R. G., Canadell, J. G., Randerson, J. T., Jackson, R. B., Hungate, B. A., Baldocchi, D. D., et al. (2010). Biophysical considerations in forestry for climate protection. *Frontiers in ecology and the environment*, doi:10.1890/090179

Baldocchi, D., Falge, E., Gu, L., Olson, R., Hollinger, D., Running, S., et al. (2001). FLUXNET: A new tool to study the temporal and spatial variability of ecosystem-scale carbon dioxide, water vapor, and energy flux densities. *Bulletin of the American Meteorological Society*, *82*, 2415–2434, doi:10.1175/1520-0477

Betts, R. A. (2000). Offset of the potential carbon sink from boreal forestation by decreases in surface albedo. *Nature*, *408*, 187–190.

Betts, R. A., Falloon, P. D., Goldewijk, K. K., & Ramankutty, N. (2007). Biogeophysical effects of land use on climate: Model simulations of radiative forcing and large-scale temperature change. *Agricultural and Forest Meteorology*, *142*, 216–233.

Bird, D. N., Kunda, M., Mayer, A., Schlamadinger, B., Canella, L., & Johnston, M. (2008). Incorporating changes in albedo in estimating the climate mitigation benefits of land use change projects. *Biogeosciences Discuss*, *5*, 1511–1543.

Bonan, G. B. (2008). Forests and climate change: Forcings, feedbacks, and the climate benefits of forests. *Science*, *320*, 1444–1449.

Cescatti, A. (1998). Effects of needle clumping in shoots and crowns on the radiative regime of a Norway spruce canopy. *Annals of Forest Science*, *55*, 89–102.

Chapin, F. S., Randerson, J. T., McGuire, A. D., Foley, J. A., & Field, C. B. (2008). Changing feedbacks in the climate–biosphere system. *Frontiers in Ecology and the Environment*, *6*, 313–320, doi:10.1890/080005

Chapin, F. S., Sturm, M., Serreze, M. C., McFadden, J. P., Key, J. R., Lloyd, A. H., et al. (2005). Role of land-surface changes in arctic summer warming. *Science*, *310*, 657–660.

Charlson, R. J., Ackerman, A. S., Bender, F. A. M., Anderson, T. L., & Liu, Z. (2007). On the climate forcing consequences of the albedo continuum between cloudy and clear air. *Tellus Series B: Chemical and Physical Meteorology*, *59*, 715–727, doi:10.1111/j.1600-0889.2007.00297

Charney, J., Quirk, W. J., Chow, S. H., & Kornfield, J. (1977). A comparative study of the effects of albedo change on drought in semi-arid regions. *Journal of the Atmospheric Sciences*, *34*, 1366–1385.

Chen, J. M., Leblanc, S. G., Cihlar, J. C., Bicheron, P., Leroy, M., Deering, D., et al. (1997). Studies of BRDF in conifer and deciduous boreal forests using the 4-scale model and airborne POLDER and ground-based PARABOLA measurements. *Geoscience and remote sensing, 1997. IGARSS '97. Remote sensing — A scientific vision for sustainable development, 1997 IEEE International* (pp. 165–167). vol.161.

Chen, J. M., Leblanc, S. G., Miller, J. R., Freemantle, J., Loechel, S. E., Walthall, C. L., et al. (1999). Compact Airborne Spectrographic Imager (CASI) used for mapping biophysical parameters of boreal forests. *Journal of Geophysical Research*, *104*, 27945–27958.

Chen, Y. M., Liang, S., Wang, J., Kim, H. Y., & Martonchik, J. V. (2008). Validation of MISR land surface broadband albedo. *International Journal of Remote Sensing*, *29*, 6971–6983, doi:10.1080/01431160802199876

Davidson, A., & Wang, S. S. (2004). The effects of sampling resolution on the surface albedos of dominant land cover types in the North American boreal region. *Remote Sensing of Environment*, *93*, 211–224, doi:10.1016/j.rse.2004.07.005

Dickinson, R. E. (1983). Land surface processes and climate surface albedos and energybalance. *Advances in Geophysics*, *25*, 305–353.

Diner, D. J., Barge, L. M., Bruegge, C. J., Chrien, T. G., Conel, J. E., Eastwood, M. L., et al. (1998). The Airborne Multi-angle Imaging SpectroRadiometer (AirMISR): Instrument description and first results. *Geoscience and Remote Sensing, IEEE Transactions on*, *36*, 1339–1349.

Dirmeyer, P. A., & Shukla, J. (1994). Albedo as a modulator of climate response to tropical deforestation. *Journal of Geophysical Research*, *99*, 20863–20877.

Frida A-M, B., Henning, R., Robert, J. C., Annica, M. L. E., & Norman, L. (2006). 22 views of the global albedo — Comparison between 20 GCMs and two satellites. *Tellus A*, *58*, 320–330.

Gao, F., Schaaf, C. B., Strahler, A. H., Roesch, A., Lucht, W., & Dickinson, R. (2005). MODIS bidirectional reflectance distribution function and albedo Climate Modeling Grid products and the variability of albedo for major global vegetation types. *Journal of Geophysical Research—Atmospheres*, *110*, D01104, doi:10.1029/2004jd005190

Gatebe, C. K., King, M. D., Platnick, S., Arnold, G. T., Vermote, E. F., & Schmid, B. (2003). Airborne spectral measurements of surface–atmosphere anisotropy for several surfaces and ecosystems over southern Africa. *Journal of Geophysical Research*, *108*, 8489.

Govaerts, Y., & Lattanzio, A. (2008). Estimation of surface albedo increase during the eighties Sahel drought from Meteosat observations. *Global and Planetary Change*, *64*, 139–145.

Hall, A., & Qu, X. (2006). Using the current seasonal cycle to constrain snow albedo feedback in future climate change. *Geophysical Research Letters*, *33*, doi:10.1029/2005gl025127

Henderson-Sellers, A., & Wilson, M. F. (1983). Surface albedo data for climatic modeling. *Reviews of Geophysics*, *21*, 1743–1778.

Holben, B. N., Eck, T. F., Slutsker, I., Tanré, D., Buis, J. P., Setzer, A., et al. (1998). AERONET —A federated instrument network and data archive for aerosol characterization. *Remote Sensing of Environment*, *66*, 1–16.

Hollinger, D. Y., Ollinger, S. V., Richardson, A. D., Meyers, T. P., Dail, D. B., Martin, M. E., et al. (2009). Albedo estimates for land surface models and support for a new paradigm based on foliage nitrogen concentration. *Global Change Biology*, *16*, 696–710.

Jin, Y. F., Schaaf, C. B., Gao, F., Li, X. W., Strahler, A. H., Lucht, W., et al. (2003a). Consistency of MODIS surface bidirectional reflectance distribution function and albedo retrievals: 1. Algorithm performance. *Journal of Geophysical Research—Atmospheres*, *108*, doi:10.1029/2002jd002803

Jin, Y., Schaaf, C. B., Woodcock, C. E., Gao, F., Li, X., Strahler, A. H., et al. (2003b). Consistency of MODIS surface bidirectional reflectance distribution function and albedo retrievals: 2 Validation. *Journal of Geophysical Research*, *108*, doi:10.1029/2002JD002804

Lawrence, D. M., & Slingo, J. M. (2004). An annual cycle of vegetation in a GCM. Part II: Global impacts on climate and hydrology. *Climate Dynamics*, *22*, 107–122, doi:10.1007/s00382-003-0367-8

Liang, S. L., Fang, H. L., Chen, M. Z., Shuey, C. J., Walthall, C., Daughtry, C., et al. (2002). Validating MODIS land surface reflectance and albedo products: Methods and preliminary results. *Remote Sensing of Environment*, *83*, 149–162.

Liu, J., Schaaf, C., Strahler, A., Jiao, Z., Shuai, Y., Zhang, Q., et al. (2009). Validation of Moderate Resolution Imaging Spectroradiometer (MODIS) albedo retrieval algorithm: Dependence of albedo on solar zenith angle. *Journal of Geophysical Research*, *114*, D01106.

Lucht, W., Hyman, A. H., Strahler, A. H., Barnsley, M. J., Hobson, P., & Muller, J. P. (2000). A comparison of satellite-derived spectral albedos to ground-based broadband albedo measurements modeled to satellite spatial scale for a semidesert landscape. *Remote Sensing of Environment*, *74*, 85–98.

Lucht, W., Schaaf, C. B., & Strahler, A. H. (2000). An algorithm for the retrieval of albedo from space using semiempirical BRDF models. *IEEE Transactions on Geoscience and Remote Sensing*, *38*, 977–998.

Masuoka, E., Tilmes, C., Gang, Y., & Devine, N. (2000). Producing global science products for the MODerate resolution Imaging Spectroradiometer (MODIS) in MODAPS. *Geoscience and Remote Sensing Symposium, 2000. Proceedings. IGARSS 2000. IEEE 2000 International* (pp. 2050–2052). vol.2055.

Masuoka, E., Wolfe, R., Sinno, S., Gang, Y., & Teague, M. (2007). A disk-based system for producing and distributing science products from MODIS. *Geoscience and Remote Sensing Symposium, 2007. IGARSS 2007. IEEE International* (pp. 3043–3046).

Moody, Eric G., King, Michael D., Schaaf, Crystal B., & Platnick, Steven G. (2008). MODIS-derived spatially complete surface albedo products: Spatial and temporal pixel distribution and zonal averages. *Journal of Applied Meteorology and Climatology*, *47*, 2879–2894.

Myhre, G., Kvalevåg, M. M., & Schaaf, C. B. (2005). Radiative forcing due to anthropogenic vegetation change based on MODIS surface albedo data. *Geophysical Research Letters*, *32*, L21410.

Ollinger, S. V., Richardson, A. D., Martin, M. E., Hollinger, D. Y., Frolking, S. E., Reich, P. B., et al. (2008). Canopy nitrogen, carbon assimilation, and albedo in temperate and boreal forests: Functional relations and potential climate feedbacks. *Proceedings of the National Academy of Sciences of the United States of America*, *105*, 19336–19341.

Pinty, B., Andredakis, I., Clerici, M., Kaminski, T., Taberner, M., Verstraete, M. M., et al. (2011). Exploiting the MODIS albedos with the two-stream inversion package (JRC-TIP): 1. Effective leaf area index, vegetation, and soil properties. *Journal of Geophysical Research*, *116*, D09105.

Pinty, B., Taberner, M., Haemmerle, V. R., Paradise, S. R., Vermote, E., Verstraete, M. M., et al. (2011). Global-scale comparison of MISR and MODIS land surface albedos. *Journal of Climate*, *24*, 732–749, doi:10.1175/2010JCLI3709.1

Pirazzini, R. (2004). Surface albedo measurements over Antarctic sites in summer. *Journal of Geophysical Research*, *109*, D20118.

Pirazzini, R., Vihma, T., Granskog, M. A., & Cheng, B. (2006). Surface albedo measurements over sea ice in the Baltic Sea during the spring snowmelt period. *Annals of Glaciology*, *44*, 7–14.

Randerson, J. T., Liu, H., Flanner, M. G., Chambers, S. D., Jin, Y., Hess, P. G., et al. (2006). The impact of boreal forest fire on climate warming. *Science*, *314*, 1130–1132, doi:10.1126/science.1132075

Román, M. O., Schaaf, C. B., Lewis, P., Gao, F., Anderson, G. P., Privette, J. L., et al. (2010). Assessing the coupling between surface albedo derived from MODIS and the fraction of diffuse skylight over spatially-characterized landscapes. *Remote Sensing of Environment*, *114*, 738–760.

Román, M. O., Schaaf, C. B., Woodcock, C. E., Strahler, A. H., Yang, X., Braswell, R. H., et al. (2009). The MODIS (Collection V005) BRDF/albedo product: Assessment of spatial representativeness over forested landscapes. *Remote Sensing of Environment*, *113*, 2476–2498.

Rotenberg, E., & Yakir, D. (2010). Contribution of semi-arid forests to the climate system. *Science*, *327*, 451–454, doi:10.1126/science.1179998

Running, S. W., Loveland, T. R., Pierce, L. L., Nemani, R. R., & Hunt, E. R. (1995). A remote sensing based vegetation classification logic for global land cover analysis. *Remote Sensing of Environment*, *51*, 39–48.

Salomon, J. G., Schaaf, C. B., Strahler, A. H., Feng, G. A. O., & Yufang Jin, G. (2006). Validation of the MODIS bidirectional reflectance distribution function and albedo retrievals using combined observations from the Aqua and Terra platforms. *IEEE Transactions on Geoscience and Remote Sensing*, *44*, 1908–1925.

Salomonson, V. V., Barnes, W. L., Maymon, P. W., Montgomery, H. E., & Ostrow, H. (1989). MODIS — Advanced facility instrument for studies of the earth as a system. *IEEE Transactions on Geoscience and Remote Sensing*, *27*, 145–153.

Schaaf, C. B., Gao, F., Strahler, A. H., Lucht, W., Li, X. W., Tsang, T., et al. (2002). First operational BRDF, albedo nadir reflectance products from MODIS. *Remote Sensing of Environment*, *83*, 135–148.

Sellers, P. J., Hall, F. G., Kelly, R. D., Black, A., Baldocchi, D., Berry, J., et al. (1997). BOREAS in 1997: Experiment overview, scientific results, and future directions. *Journal of Geophysical Research—Atmospheres*, *102*, 28731–28769.

Stroeve, J., Box, J. E., Gao, F., Liang, S., Nolin, A., & Schaaf, C. (2005). Accuracy assessment of the MODIS 16-day albedo product for snow: comparisons with Greenland in situ measurements. *Remote Sensing of Environment*, *94*, 46–60.

Susaki, J., Yasuoka, Y., Kajiwara, K., Honda, Y., & Hara, K. (2007). Validation of MODIS albedo products of paddy fields in Japan. *Geoscience and Remote Sensing, IEEE Transactions on*, *45*, 206–217.

Tian, Y., Dickinson, R. E., Zhou, L., Myneni, R. B., Friedl, M., Schaaf, C. B., et al. (2004). Land boundary conditions from MODIS data and consequences for the albedo of a climate model. *Geophysical Research Letters*, *31*, L05504.

Tittebrand, A., Spank, U., & Bernhofer, C. H. (2009). Comparison of satellite- and ground-based NDVI above different land-use types. *Theoretical and Applied Climatology*, *98*, 171–186.

Vavrus, S., Ruddiman, W. F., & Kutzbach, J. E. (2008). Climate model tests of the anthropogenic influence on greenhouse-induced climate change: The role of early human agriculture, industrialization, and vegetation feedbacks. *Quaternary Science Reviews*, *27*, 1410–1425.

Wang, K., Liang, S., Schaaf, C. L., & Strahler, A. H. (2010). Evaluation of Moderate Resolution Imaging Spectroradiometer land surface visible and shortwave albedo products at FLUXNET sites. *Journal of Geophysical Research*, *115*, D17107.